PROGRESS IN COLOR, COLORANTS AND COATINGS

available online @ www.pccc.icrc.ac.ir

Prog. Color Colorants Coat. 8 (2015), 177-196

Ministry of Science, Research and Technology
Institute for Color Science and Technology

Electrochemical Assessment of Imidazole Derivatives as Corrosion Inhibitors for Mild Steel in 3.5% NaCl Solution

M. Mahdavian [*1] and M. M. Attar [*2]

[1.] Assistant Professor, Surface Coating and Corrosion Department, Institute for Color Science and Technology, P. O. Box 16765-654, Tehran, Iran.

[2.] Professor, Polymer Engineering and Color Technology Department, Amirkabir University of Technology, P. O. Box: 15875-4413, Tehran, Iran.

ARTICLE INFO

Article history:
Received: 17-04-2015
Final Revised: 24-05-2015
Accepted: 31-05-2015
Available online: 31-05-2015

Keywords:
Adsorption
Corrosion
Polarization
EIS

ABSTRACT

The corrosion inhibition efficiency of benzimidazole, 2-methylbenzimidazole and 2- aminobenzimidazole for mild steel immersed in 3.5% NaCl solution was investigated by electrochemical impedance spectroscopy at concentration range from 10^{-5} to 10^{-2} M of imidazoles and temperature range from 30 to 50 °C. In addition, DC polarization was examined to determine inhibition mechanism at concentration range from 10^{-5} to 10^{-2} M of the imidazole derivatives. Double layer capacitance and charge transfer resistance were extracted from EIS plots after fitting with an appropriate circuit. Surface coverage was calculated based on capacitance and resistance of the corroding cell. It was found that increase of inhibitor concentration and temperature results in increase and decrease of surface coverage, respectively. The results showed that these compounds have limited corrosion inhibition. The adsorption of these compounds on the steel surface obeys Temkin isotherm. Prog. Color Colorants Coat. 8 (2015), 177-196 © Institute for Color Science and Technology.

1. Introduction

Mild steel is used in a wide range of industrial applications as a main structure. Corrosion occurs due to instability of steel in corrosive media. Organic corrosion inhibitors have found their place in corrosion protection as an effective option for different corrosive media. Imidazoles have two nitrogen atoms in their heterocyclic ring which are pyrrole (1N) and pyridine (3N) like nitrogen atoms (Figure 1). Possible anchoring sites to form chemical bonding with metal surface are nitrogen atoms with lone pair of electrons and aromatic ring [1]. Some imidazoles are widely used to protect steel in acidic media [2-11]. However, few investigations have been done to evaluate their protection in corrosive neutral condition [12, 13].

Increased solubility of corrosion products below pH 5 can make the major difference between inhibition at

*Corresponding author: mahdavian-m@icrc.ac.ir and attar@aut.ac.ir

neutral and acidic condition. Presence of rust on mild steel surface can provide further adsorption sites for corrosion inhibitors.

An adsorption isotherm represents a functional relationship between the amount of adsorbate at an interface and the activity of adsorbate in the solution. Adsorption isotherms give some information such as free energy of adsorption, the character of adsorption layer and the interaction between adsorbed species. The following adsorption isotherms are commonly used to study mechanism of corrosion inhibition [14-18]:

$$\text{Langmuir: } \frac{C_{inh}}{55.5}\exp\left(\frac{-\Delta G^{0}_{ads}}{RT}\right) = \frac{\theta}{1-\theta} \quad (1)$$

Bockris-Swinkels:

$$\frac{C_{inh}}{55.5}\exp\left(\frac{-\Delta G^{0}_{ads}}{RT}\right) = \frac{\theta}{(1-\theta)^{x}}\frac{[\theta + x(1-\theta)]^{x-1}}{x^{x}} \quad (2)$$

$$\text{Frumkin: } \frac{C_{inh}}{55.5}\exp\left(\frac{-\Delta G^{0}_{ads}}{RT}\right) = \frac{\theta}{1-\theta}\exp(f\theta) \quad (3)$$

$$\text{Temkin: } \frac{C_{inh}}{55.5}\exp\left(\frac{-\Delta G^{0}_{ads}}{RT}\right) = \exp(f\theta) \quad (4)$$

$$\text{Freundlich: } \frac{C^{f}_{inh}}{55.5}\exp\left(\frac{-\Delta G^{0}_{ads}}{RT}\right) = \theta \quad (5)$$

where C_{inh} represents the concentration of inhibitor, ΔG^{0}_{ads} the standard free energy of adsorption, R the universal gas constant, T the absolute temperature and θ the surface coverage. Parameter x in Eq. (2) is the number of adsorbed water molecules replaced by a molecule of inhibitor. Parameter f in Frumkin, Temkin and Freundlich isotherms is called "interaction parameter", "surface heterogeneity" and “adsorption intensity”, respectively.

The basic isotherm for adsorption of ions or molecular species upon electrodes is that of Langmuir. Langmuir fails to consider the energy needed for the displacement of water by inhibitor molecule, the fact that is taken into account in Bockris-Swinkels isotherm [18]. Langmuir adsorption isotherm should only be applicable to surfaces which are uniform in respect to the adsorption sites and where the adsorbed entities are too far apart to interact significantly [19]. Frumkin’s isotherm allows attraction and repulsion between adsorbed entities; however, it fails to take into consideration the surface heterogeneity (i.e. sites of varying adsorptive power) of the solid surface [19]. Freundlich isotherm, previously considered being an empirical isotherm, unlike the Langmuir isotherm does not indicate an adsorption limit [20]. In other words, Freundlich model is based on the assumption that there is no limiting concentration of adsorbate as solution concentration increases without limit [20].

Surface coverage (θ) could be obtained from different methods including weight loss measurement and electrochemical AC & DC methods [21-23]. Electrochemical parameters could be extracted by electrochemical impedance spectroscopy (EIS) results modeling with an appropriate circuit. Extracted parameters could be used in studying corrosion protection performance of inhibitors, organic and inorganic coatings [24-28]. In this paper, utilizing EIS, inhibition of imidazole derivatives at different concentrations and temperatures was measured and the best adsorption isotherm was evaluated. In addition, DC polarization was used to evaluate the inhibition mechanism.

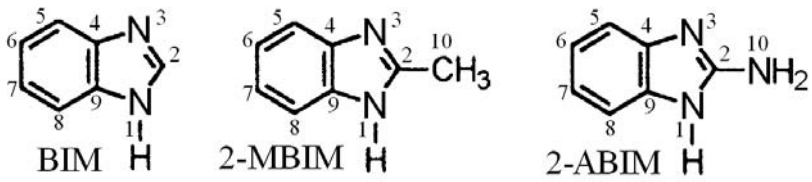

Figure 1: Structure of corrosion inhibitors.

2. Experimental

A 3.5% NaCl solution was prepared from laboratory grade NaCl and distilled water. Three imidazole derivatives including benzimidazole (BIM), 2- methyl benzimidazole (2-MBIM) and 2-amino benzimidazole (2-ABIM) were obtained from Merck and used without further purification. Test solutions were prepared in four different concentrations of imidazole derivatives in 3.5% NaCl solution. Concentrations under study were 10^{-2}, 10^{-3}, 10^{-4}, and 10^{-5} M. An isothermal water bath was used in order to maintain the temperature precisely at three temperatures: 30, 40 and 50 ℃ within ±0.1 ℃ variance. Mild steel (CK15) sheets of 2 mm thickness were obtained from Mobarakeh Steel Company and cut down to 2.5×7 cm^2 samples. Samples were abraded with a magnetic abrader to remove mill scale of the surface, followed by degreasing with xylene and acetone. Surface roughness of the abraded surface was in the range of 1-5 microns peak-to-valley measured by Elcometer 223. An area of 1 cm^2 of samples was exposed to the electrolytes whilst other areas of the plates were sealed with beeswax-colophony mixture. Each specimen was immersed in 100ml of prepared electrolytes and EIS measurements were carried out using Autolab PGSTAT12 after 24 hours of immersion. EIS was implemented at open circuit potential at frequency range of 10^{-2}–10^{+4} Hz with 10 mV perturbation. Reference electrode and counter electrode were silver–silver chloride and platinum, respectively.

DC polarization was examined on mild steel samples using Autolab PGSTAT12 at 1 mV/s scan rate after 24 hr of immersion in test solutions at 30 ℃. The effect of imidazole derivatives on the pH of the solutions was assessed by pH-meter of WTW model pH-315i for the solutions containing 10^{-2} M of the inhibitors and Blank solution.

FT-IR of corrosion products on the mild steel surface after 24-hr immersion in 10^{-2} M of the inhibitors was evaluated. Infrared spectra were obtained with a Bomem FT-IR 2000 spectrophotometer in the range of 4000–400 cm^{-1}.

3. Results and discussion

3.1. Electrochemical impedance spectroscopy

All impedance spectra were measured at the respective corrosion potential. The results are shown in Figure 2-4. The EIS results were analyzed in terms of the equivalent circuit shown in Figure 5. Generally, this circuit falls into the classic parallel capacitor and resistor combination. FRA software (version 4.9.005 beta) of Autolab is used for impedance data analysis. The electrical elements in this figure are R_s, R_{ct} and CPE_{dl} which represent electrolyte resistance, charge transfer resistance at metal electrolyte interface and non-ideal double layer capacitance, respectively. The capacitance values were calculated according to the following equation [29]:

$$C_{dl} = \frac{\left(Y_0 R_{ct}\right)^{1/n}}{R_{ct}} \quad (6)$$

In Eq. (6), C_{dl} represents double layer capacitance, Y_0 the magnitude of admittance of CPE, n the exponential term and R_{ct} the charge transfer resistance. Surface coverage values were calculated by Eq. (7) and (8) [30].

$$\theta_R = \frac{R_{ct}\left(\text{with inhibitor}\right) - R_{ct}\left(\text{without inhibitor}\right)}{R_{ct}\left(\text{with inhibitor}\right)} \quad (7)$$

$$\theta_C = \frac{C_{dl}\left(\text{without inhibitor}\right) - C_{dl}\left(\text{with inhibitor}\right)}{C_{dl}\left(\text{without inhibitor}\right)} \quad (8)$$

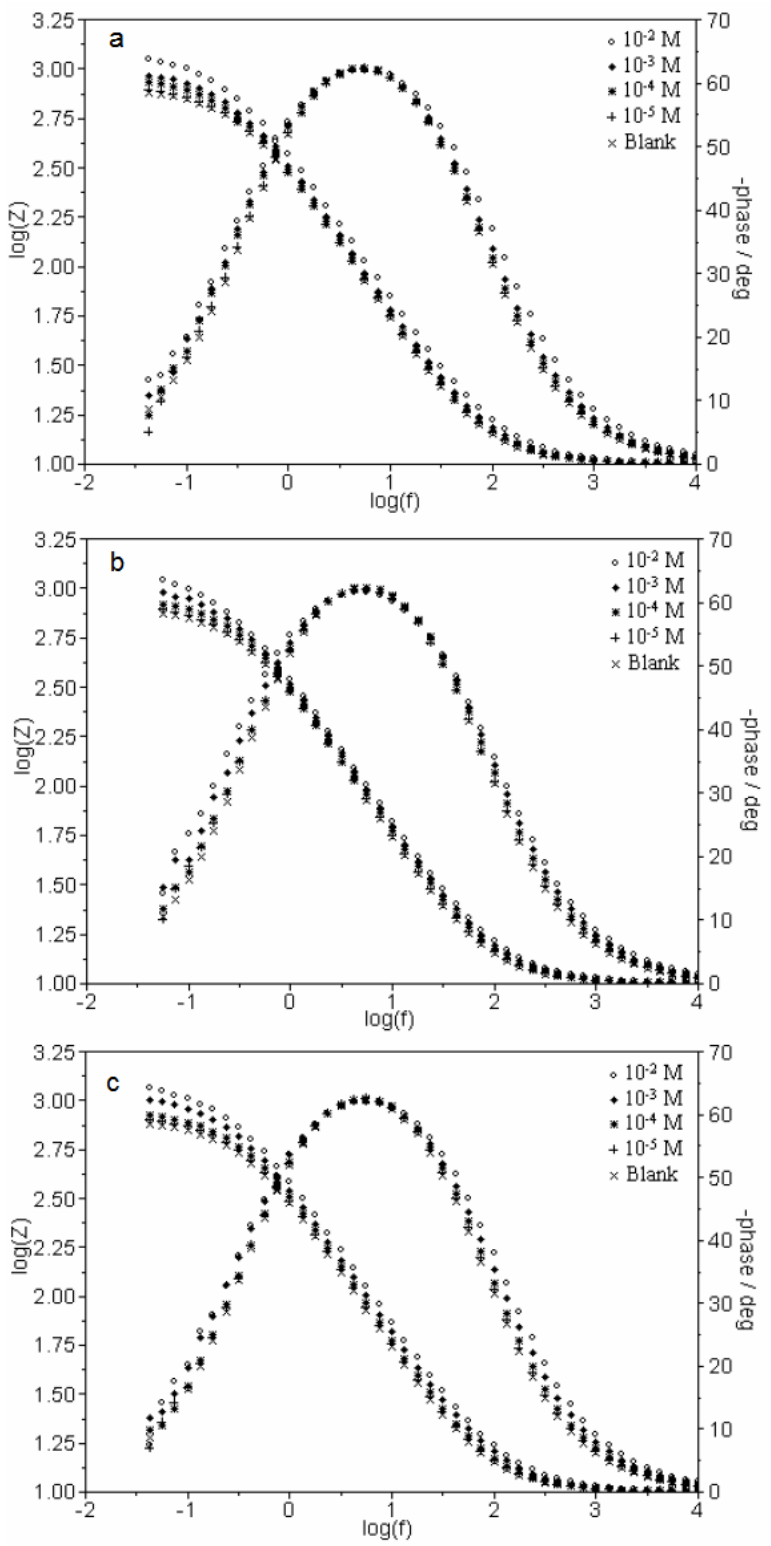

Figure 2: EIS Bode diagrams of mild steel samples immersed in 3.5% NaCl solution containing BIM (a), 2-MBIM (b), 2-ABIM (c) for 24 hr at 30 ºC.

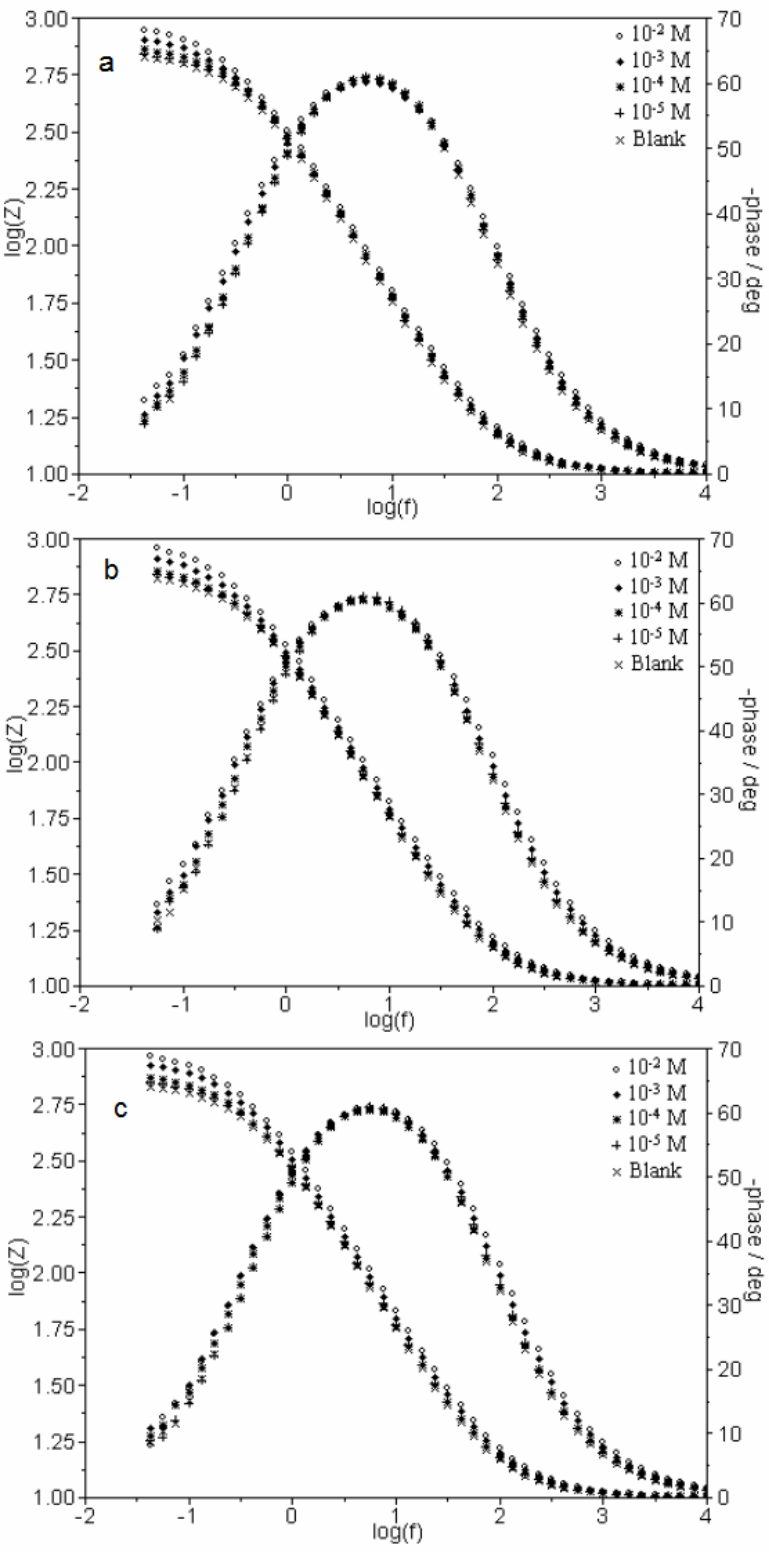

Figure 3: EIS Bode diagrams of mild steel samples immersed in 3.5% NaCl solution containing BIM (a), 2-MBIM (b), 2-ABIM (c) for 24 hr at 40 ºC.

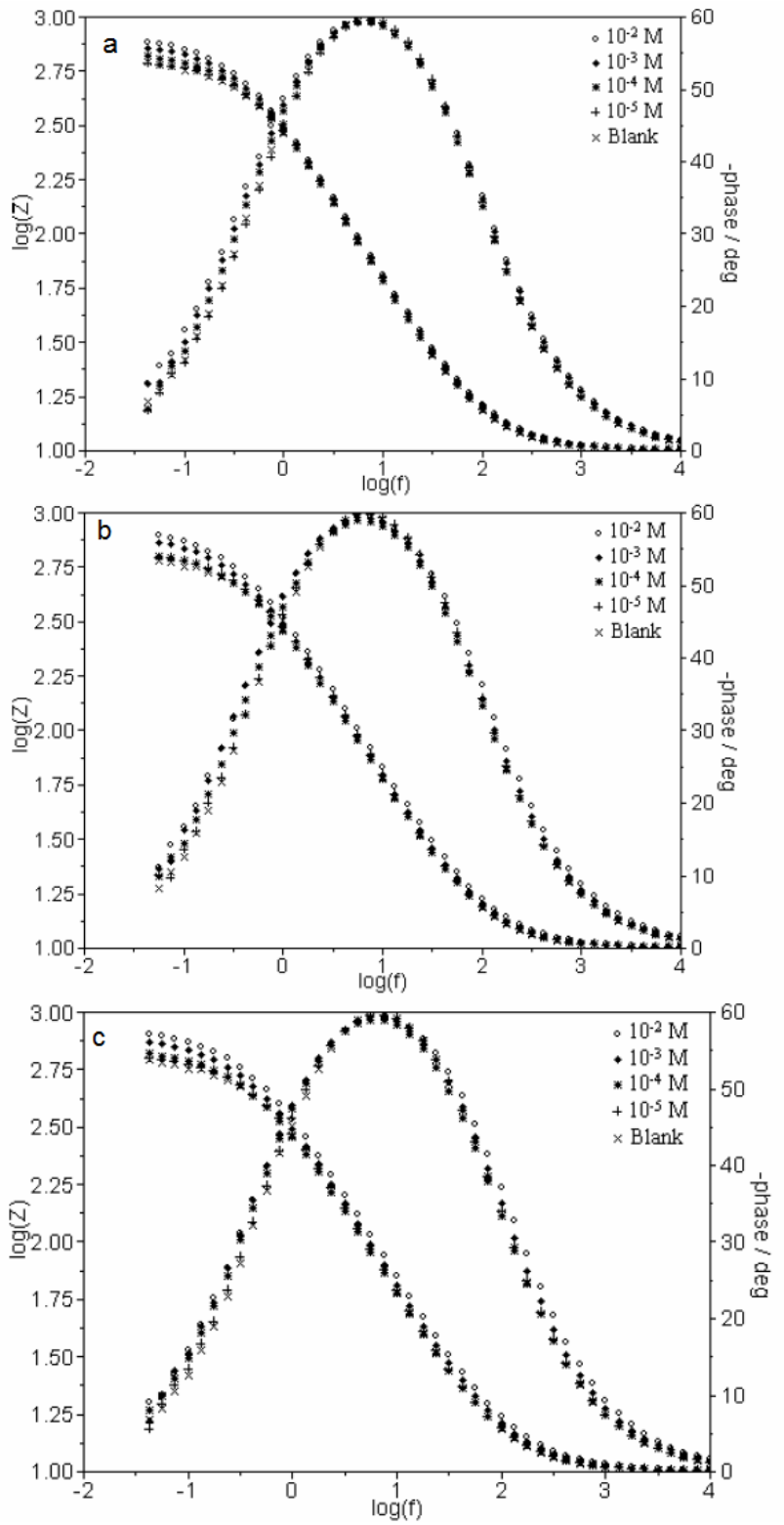

Figure 4: EIS Bode diagrams of mild steel samples immersed in 3.5% NaCl solution containing BIM (a), 2-MBIM (b), 2-ABIM (c) for 24 hr at 50 ºC.

Typical Bode diagrams after fitting with electrical model (Figure 5) are presented in Figure 6. All parameters were extracted for each specimen and the results are listed in Table 1.

As it can be understood from Table 1, charge transfer resistance increases with increase of concentration and decrease of temperature. Simultaneously, double layer capacitance goes in opposite direction with charge transfer resistance. Increase of charge transfer resistance in the presence of inhibitors can be related to surface coverage of these molecules. Double layer capacitance decline can be related to the decrease of dielectric constant or increase of double layer thickness. The inhibition of the inhibitors increases in the order 2-ABIM> 2-MBIM>BIM.

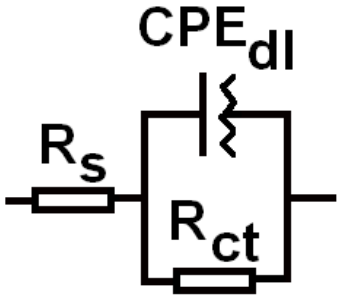

Figure 5: Electrical circuit model used to fit EIS results with one time constant.

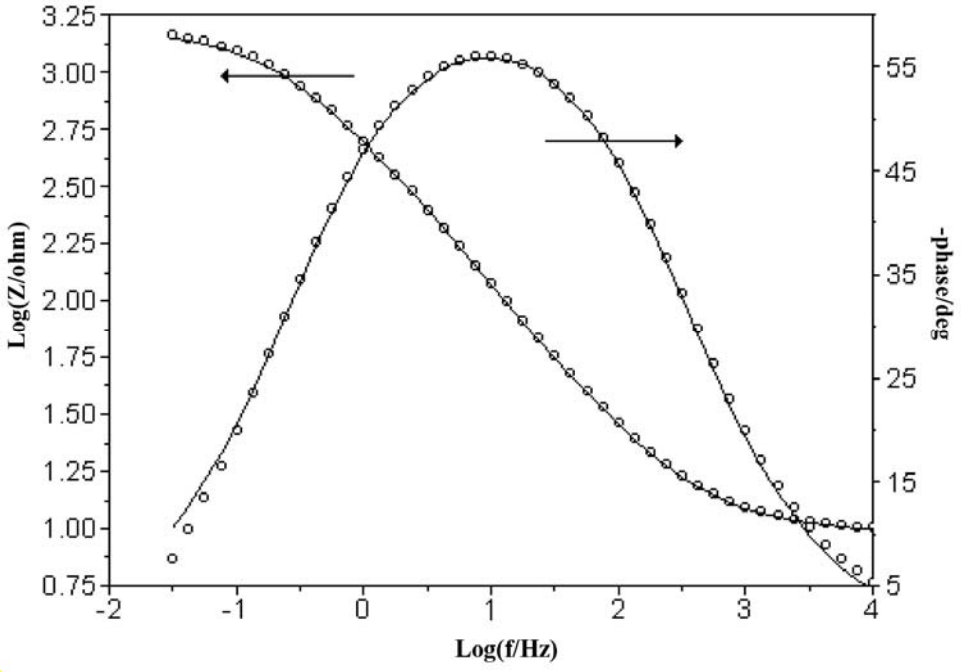

Figure 6: Bode diagram resulted from fitting of EIS results for CK15 samples immersed for 1 day at 30ºC in 3.5% NaCl in presence of 0.01 M BIM: Extracted elements from fitting were R_{ct}=1550.9 Ohm.cm^2, Y_{0dl}=1.96×10^{-5} Ω^{-1}.cm^{-2}, n_{dl}=0.711.

Table 1: Electrochemical parameters extracted from EIS of the samples after 24-hr immersion in test solutions.

Imidazole Derivatives	Temperature	Inhibitor Concentration	R_{ct} (Ωcm^2)	Y_{0dl} ($\Omega^{-1}cm^{-2}$)	n_{dl}	C_{dl} (Fcm^{-2})	θ_R(%)	θ_C(%)
BIM	30 ˚C	10^{-2} M	1550.9	1.96×10^{-5}	0.711	4.73×10^{-6}	43.38	90.12
		10^{-3} M	1218.1	5.17×10^{-5}	0.762	2.17×10^{-5}	27.91	54.60
		10^{-4} M	1111.0	6.19×10^{-5}	0.781	2.93×10^{-5}	20.96	38.89
		10^{-5} M	947.4	8.18×10^{-5}	0.802	4.36×10^{-5}	7.31	8.99
	40 ˚C	10^{-2} M	1180.0	5.98×10^{-5}	0.672	1.64×10^{-5}	36.62	67.32
		10^{-3} M	1010.0	6.19×10^{-5}	0.761	2.59×10^{-5}	25.97	48.35
		10^{-4} M	862.1	8.19×10^{-5}	0.776	3.82×10^{-5}	13.25	23.97
		10^{-5} M	804.5	9.62×10^{-5}	0.788	4.83×10^{-5}	7.04	3.70
	50 ˚C	10^{-2} M	958.1	9.08×10^{-5}	0.665	2.66×10^{-5}	31.80	40.51
		10^{-3} M	857.1	9.22×10^{-5}	0.699	3.10×10^{-5}	23.79	30.62
		10^{-4} M	742.6	9.12×10^{-5}	0.765	3.98×10^{-5}	12.01	10.87
		10^{-5} M	681.4	9.58×10^{-5}	0.778	4.40×10^{-5}	4.11	1.47
2-MBIM	30 ˚C	10^{-2} M	1579.4	1.63×10^{-5}	0.689	3.13×10^{-6}	44.40	93.46
		10^{-3} M	1314.4	6.01×10^{-5}	0.694	1.97×10^{-5}	33.19	58.97
		10^{-4} M	1083.4	6.89×10^{-5}	0.751	2.92×10^{-5}	18.95	39.11
		10^{-5} M	987.1	8.36×10^{-5}	0.784	4.20×10^{-5}	11.04	12.37
	40 ˚C	10^{-2} M	1275.0	4.01×10^{-5}	0.724	1.29×10^{-5}	41.34	74.29
		10^{-3} M	1085.2	6.54E-05	0.732	2.48×10^{-5}	31.08	50.55
		10^{-4} M	921.1	7.50×10^{-5}	0.773	3.43×10^{-5}	18.80	31.77
		10^{-5} M	814.3	9.34×10^{-5}	0.797	4.85×10^{-5}	8.15	3.39
	50 ˚C	10^{-2} M	1063.5	6.48×10^{-5}	0.730	2.41×10^{-5}	38.56	46.06
		10^{-3} M	871.1	8.14×10^{-5}	0.732	3.08×10^{-5}	24.99	31.00
		10^{-4} M	789.2	8.33×10^{-5}	0.776	3.79×10^{-5}	17.21	15.25
		10^{-5} M	696.4	9.42×10^{-5}	0.781	4.39×10^{-5}	6.17	1.87
2-ABIM	30 ˚C	10^{-2} M	1743.8	1.43×10^{-5}	0.703	3.00×10^{-6}	49.64	93.73
		10^{-3} M	1338.1	4.67×10^{-5}	0.727	1.65×10^{-5}	34.37	65.55
		10^{-4} M	1195.7	6.22×10^{-5}	0.751	2.62×10^{-5}	26.56	45.21
		10^{-5} M	1013.9	7.87×10^{-5}	0.797	4.13×10^{-5}	13.39	13.86
	40 ˚C	10^{-2} M	1302.0	4.02×10^{-5}	0.711	1.21×10^{-5}	42.56	75.89
		10^{-3} M	1043.0	5.78×10^{-5}	0.727	2.01×10^{-5}	28.29	59.94
		10^{-4} M	943.3	7.93×10^{-5}	0.750	3.35×10^{-5}	20.71	33.23
		10^{-5} M	840.3	9.37×10^{-5}	0.783	4.62×10^{-5}	10.99	7.88
	50 ˚C	10^{-2} M	1032.5	6.51×10^{-5}	0.707	2.12×10^{-5}	36.71	52.47
		10^{-3} M	892.9	6.54×10^{-5}	0.754	2.59×10^{-5}	26.82	42.13
		10^{-4} M	796.5	8.18×10^{-5}	0.770	3.62×10^{-5}	17.97	19.11
		10^{-5} M	707.7	9.25×10^{-5}	0.782	4.32×10^{-5}	7.67	3.31
Blank	30 ˚C	-	878.1	8.67×10^{-5}	0.813	4.79×10^{-5}	-	-
	40 ˚C	-	747.9	9.95×10^{-5}	0.800	5.02×10^{-5}	-	-

Table 1: Continued.

Imidazole Derivatives	Temperature	Inhibitor Concentration	R_{ct} (Ωcm^2)	Y_{0dl} ($\Omega^{-1}cm^{-2}$)	n_{dl}	C_{dl} (Fcm^{-2})	θ_R(%)	θ_C(%)
Blank	50 ˚C	-	653.4	9.67×10^{-5}	0.782	4.47×10^{-5}	-	-

Parameter n of CPE element decreases with increase of inhibitor concentration and temperature. This element (n) could be linked to surface heterogeneity [31]. It seems that more heterogeneous surfaces can be formed with adsorption of inhibitors on the surface. It is quite interesting to know this happens for all three imidazoles. This result is completely in contradiction with the results of other authors where they report more homogenous surface obtained in the presence of organic inhibitors [32-34]. This could be related to different nature of protection in acidic and neutral conditions. Increased solubility of corrosion products in strong acidic environments can make the major difference between inhibition at neutral and acidic condition. Inhibitors could adsorb on corrosion products and they may affect rust structure on the surface. This phenomenon is discussed in section 3.5.

3.2. DC polarization

The polarization curves of mild steel in 3.5% NaCl solution in the absence and presence of BIM, 2-MBIM and 2-ABIM in different concentrations are shown in Figure 7a, 7b and 7c, respectively. Corrosion potentials shift to more negative potentials and depression of cathodic polarization curve indicated that cathodic inhibition is dominant mechanism of inhibition. The inhibition efficiency (IE%) was calculated by Eq. 9.

$$IE\% = 100\frac{I_{corr}(without inhibitor) - I_{corr}(within hibitor)}{I_{corr}(without inhibitor)} \quad (9)$$

where I_{corr} is corrosion current density determined by extrapolation of Tafel lines. The calculated IE% and I_{corr} and the measured corrosion potential (E_{corr}) are listed in Table 2. The results reveal that with increasing inhibitor concentration, corrosion current density decreases and inhibition efficiency increases. The inhibition of the inhibitors increases in the order 2-MBIM≈2-ABIM>BIM. At initial immersion time, inhibition sequence is affected by the kinetic of adsorption. However, at higher exposure times, the thermodynamic of adsorption is effective on inhibition sequence of the benzimidazole derivatives. This could be the probable reason for the difference between inhibition orders obtained after 1-hr and 24-hr immersion. More discussions on inhibition sequence are provided in section 3.4.

3.3. Adsorption isotherms

Many investigators have used weight lost and potentiostatic polarization techniques to determine inhibition efficiency, which is then taken equal to surface coverage. Two methods are provided by equations 7 and 8 to determine surface coverage. In this section, we used data obtained from these two methods to determine the adsorption isotherm.

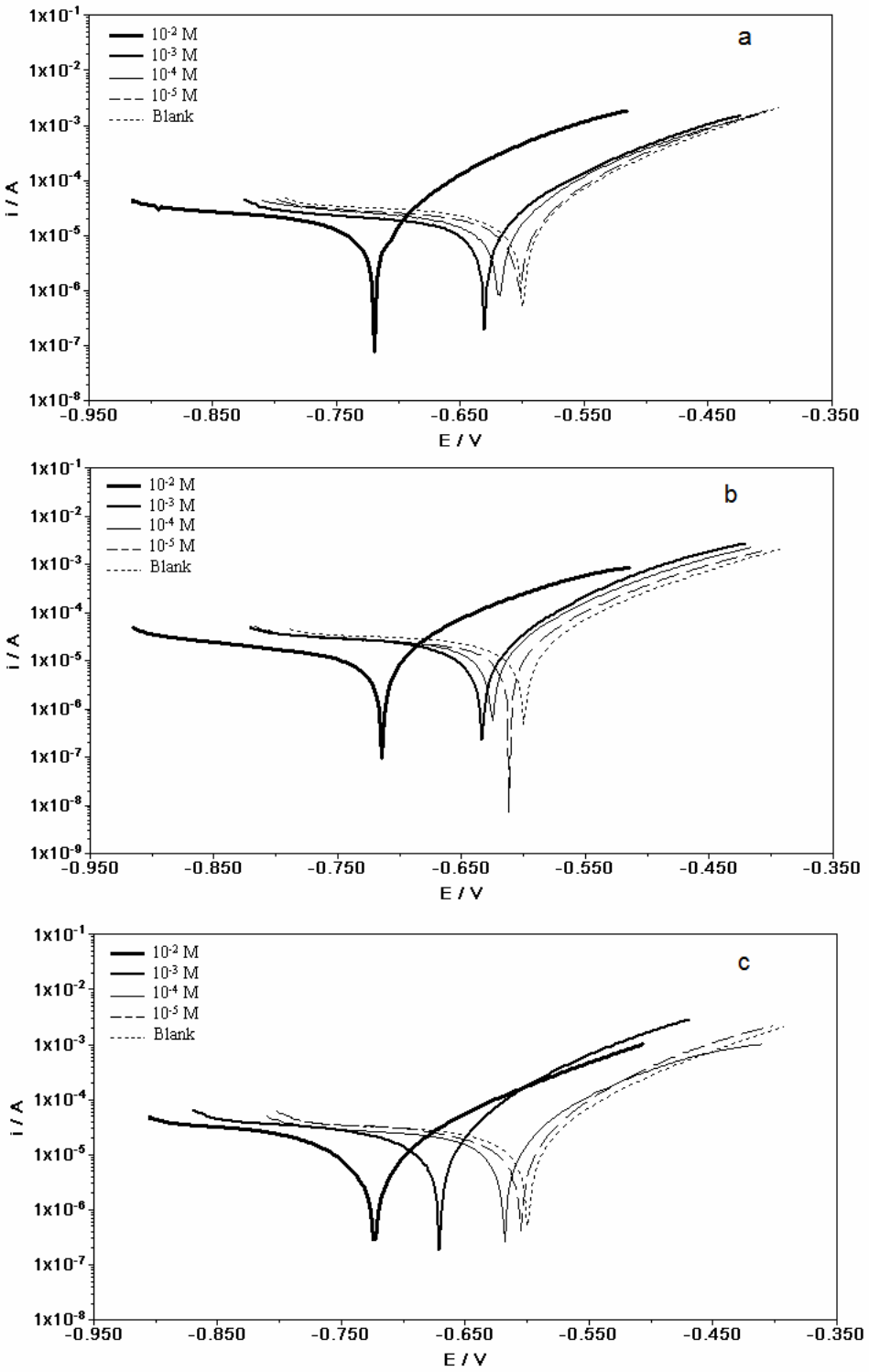

Figure 7: DC polarization curves of mild steel samples immersed in 3.5% NaCl solution containing BIM (a), 2-MBIM (b), 2-ABIM (c) for 24 hr at 30 ºC.

Table 2: Electrochemical parameters extracted from DC polarization of the samples immersed after 1hr immersion in test solutions at 30 ˚C.

Imidazole Derivatives	Inhibitor Concentration	E_{corr} (mV vs Ag/AgCl)	I_{corr} (Acm^{-2})	IE(%)
BIM	10^{-2} M	-720	1.03×10^{-5}	40.85
	10^{-3} M	-631	1.31×10^{-5}	24.93
	10^{-4} M	-618	1.55×10^{-5}	10.79
	10^{-5} M	-604	1.63×10^{-5}	6.46
2-MBIM	10^{-2} M	-714	8.88×10^{-6}	48.96
	10^{-3} M	-634	1.18×10^{-5}	32.04
	10^{-4} M	-625	1.49×10^{-5}	14.32
	10^{-5} M	-612	1.63×10^{-5}	6.18
2-ABIM	10^{-2} M	-723	9.37×10^{-6}	46.14
	10^{-3} M	-671	1.17×10^{-5}	32.61
	10^{-4} M	-618	1.51×10^{-5}	12.94
	10^{-5} M	-606	1.62×10^{-5}	6.86
Blank	-	-601	1.74×10^{-5}	-

Table 3: Extracted thermodynamic parameters based on θ_R and θ_C calculations.

Thermodynamic Parameters		BIM	2-MBIM	2-ABIM
θ_R	ΔH^0_{ads} ($kJmol^{-1}$)	-25.7	-26.1	-32.0
	ΔS^0_{ads} ($kJmol^{-1}K^{-1}$)	57.3	59.4	46.0
θ_C	ΔH^0_{ads} ($kJmol^{-1}$)	-31.0	-32.5	-36.3
	ΔS^0_{ads} ($kJmol^{-1}K^{-1}$)	33.6	30.1	21.0

3.3.1. Calculations based on θ_R

Different adsorption isotherms were examined on the results listed in Table 1. Isotherms which fit the results are summarized as follow:

Inhibitor concentrations (C_{inh}) were plotted versus C_{inh}/θ. The resulting slope of the fitted line was far beyond 1 indicating that Langmuir adsorption isotherm fails to fit the results. Same failure was occurred when Bockris–Swinkels adsorption isotherm evaluated by plotting

$$\log\left[\frac{\theta}{(1-\theta)^x}\frac{(\theta+x(1-\theta))^{x-1}}{x^x}\right] \text{ versus } \log(C_{inh})$$

This evaluation performed for x: 2 to 4 where x is the number of substituted water molecules with one inhibitor molecule. As x increased, the slope of the fitted line showed more deviation from 1. Temkin, Frumkin and Freundlich isotherms provided better results. However, the best correlation with R-square closed to 1 was obtained for Temkin isotherm. The obtained R-squares were in the range of 0.88-0.97, 0.82-0.96 and 0.83-0.96 for Temkin, Frumkin and Freundlich isotherms, respectively. Resulting fitted plots of θ versus $Ln(C_{inh})$ are illustrated in Figures 8a, 8b and 8c for the samples immersed in solutions containing BIM, 2-MBIM and 2-ABIM, respectively.

According to Temkin isotherm, Eq. (4), standard free energy of adsorption was calculated. Regarding Eq. (10), variation of enthalpy and entropy of adsorption could be extracted from the free energy of adsorption as shown in Figure 9.

$$\Delta G^{0}_{ads} = \Delta H^{0}_{ads} - T\Delta\Delta^{0}_{ads} \quad (10)$$

Resulting thermodynamic parameters are summarized in Table 3. Surface heterogeneity parameter (f value) extracted from Temkin isotherm was 20, 20.7 and 19.8 for BIM, 2-MBIM, 2-ABIM, respectively.

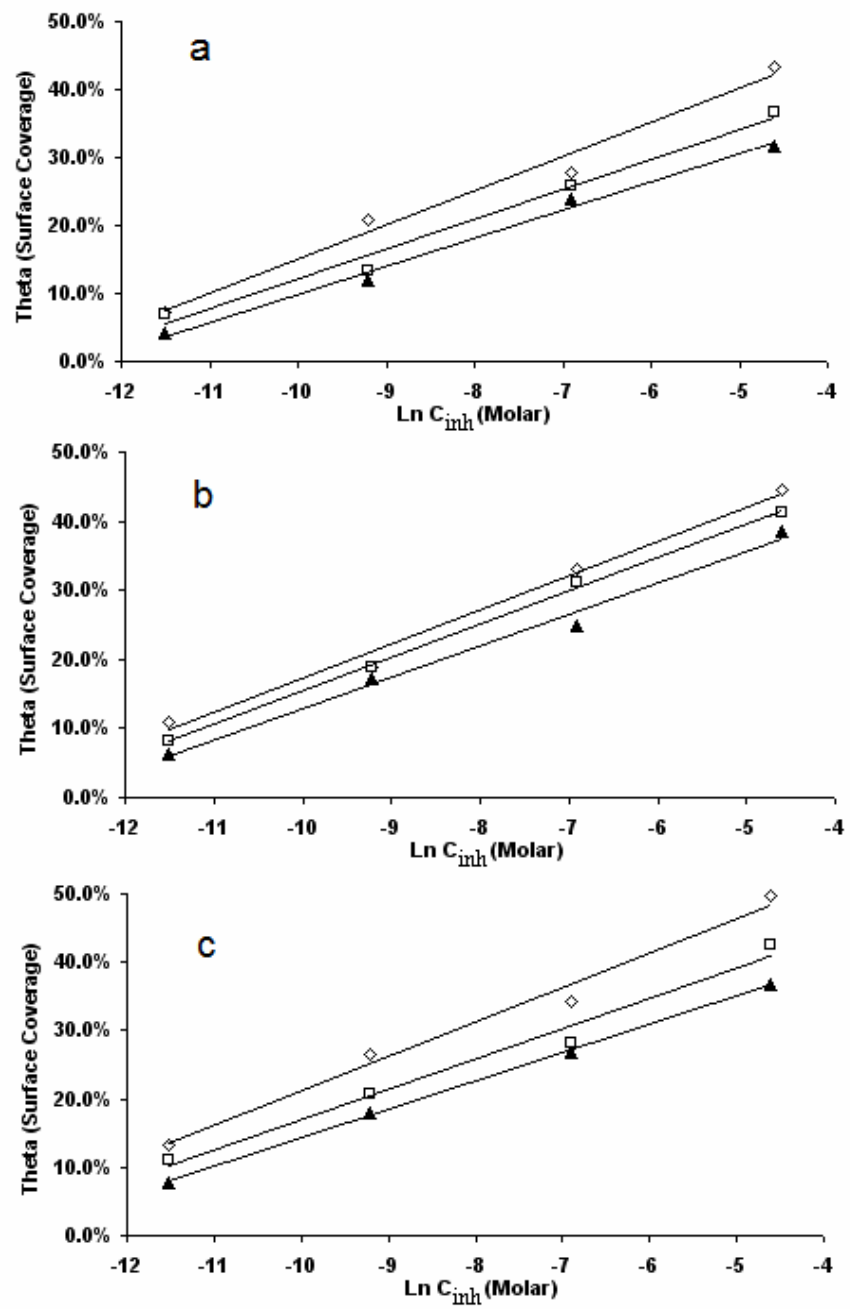

Figure 8: The relationship between surface coverage (θ_R) and Ln (C_{inh}) for BIM (a), 2-MBIM (b) and 2-ABIM (c) at different temperatures; 30 (◊), 40 (□) 50ºC (▲).

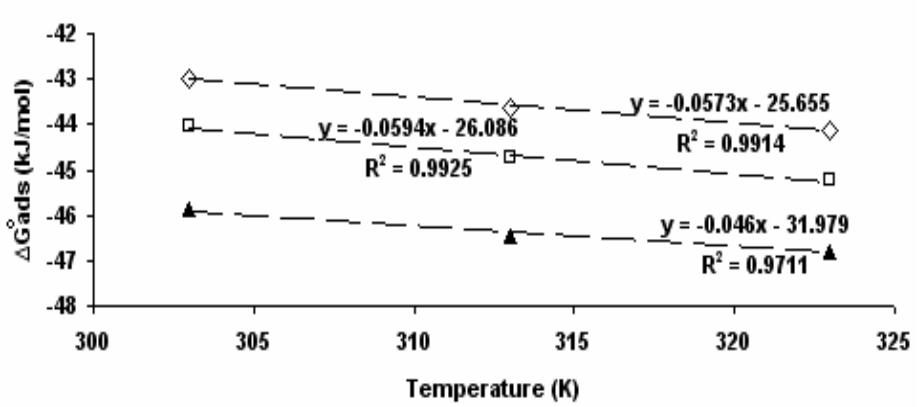

Figure 9: The relationship between ΔG^0_{ads} and temperature for BIM (◊), 2-MBIM (□) and 2-ABIM (▲) based on θ_R calculations.

3.3.2. Calculations based on θ_C

As in the case of θ_R, different adsorption isotherms were examined on the provided results in Table 1. Same failure occurred with Langmuir, Bockris–Swinkels, Freundlich and Frumkin isotherms, while Temkin displayed to be the best fitting isotherm. Resulting fitted plots of θ versus Ln (C_{inh}) are displayed in Figures 10a, 10b and 10c for the samples immersed in solutions containing BIM, 2-MBIM and 2-ABIM, respectively. According to Eq. (4), free energy of adsorption is related to the intercept and slope of these plots (Figure 10). Concerning Eq. (10), variation of enthalpy and entropy of adsorption are extracted from the free energy of adsorption as shown in Figure 11. Resulting thermodynamic parameters are summarized in Table 3. Surface heterogeneity parameter (f value) extracted from Temkin isotherm was 8.9, 8.7 and 8.9 for BIM, 2-MBIM, 2-ABIM, respectively.

The adsorption of the inhibitors is found to obey the Temkin adsorption isotherm when calculations were based on θ_R and θ_C. This is quite different from the adsorption isotherms obtained by other researchers for adsorption of benzimidazole derivatives on mild steel surface [35-38].

Abboud et al. [35] found that 2,2′-bis(benzimidazole) in 1 M HCl solution follows Langmuir isotherm. Also, Morales-Gil et al. [36] found that 2-mercaptobenzoimidazole and benzimidazole in 1 M H_2SO_4 solution follows Langmuir isotherm. Popova et al [37, 38] showed that Frumkin isotherm better describes adsorption of wide range of benzimidazole derivatives in 1 M HCl solution.

Increased solubility of corrosion products in strong acidic condition can make the major difference between inhibition at neutral and acidic condition. Presence of rust on mild steel surface in neutral condition can provide further adsorption sites for corrosion inhibitors and as a result adsorption isotherms could be different. Porous structure of ferric oxide hydroxides on mild steel surface could provide different adsorption sites with different energies on the surface which results is heterogeneous surface.

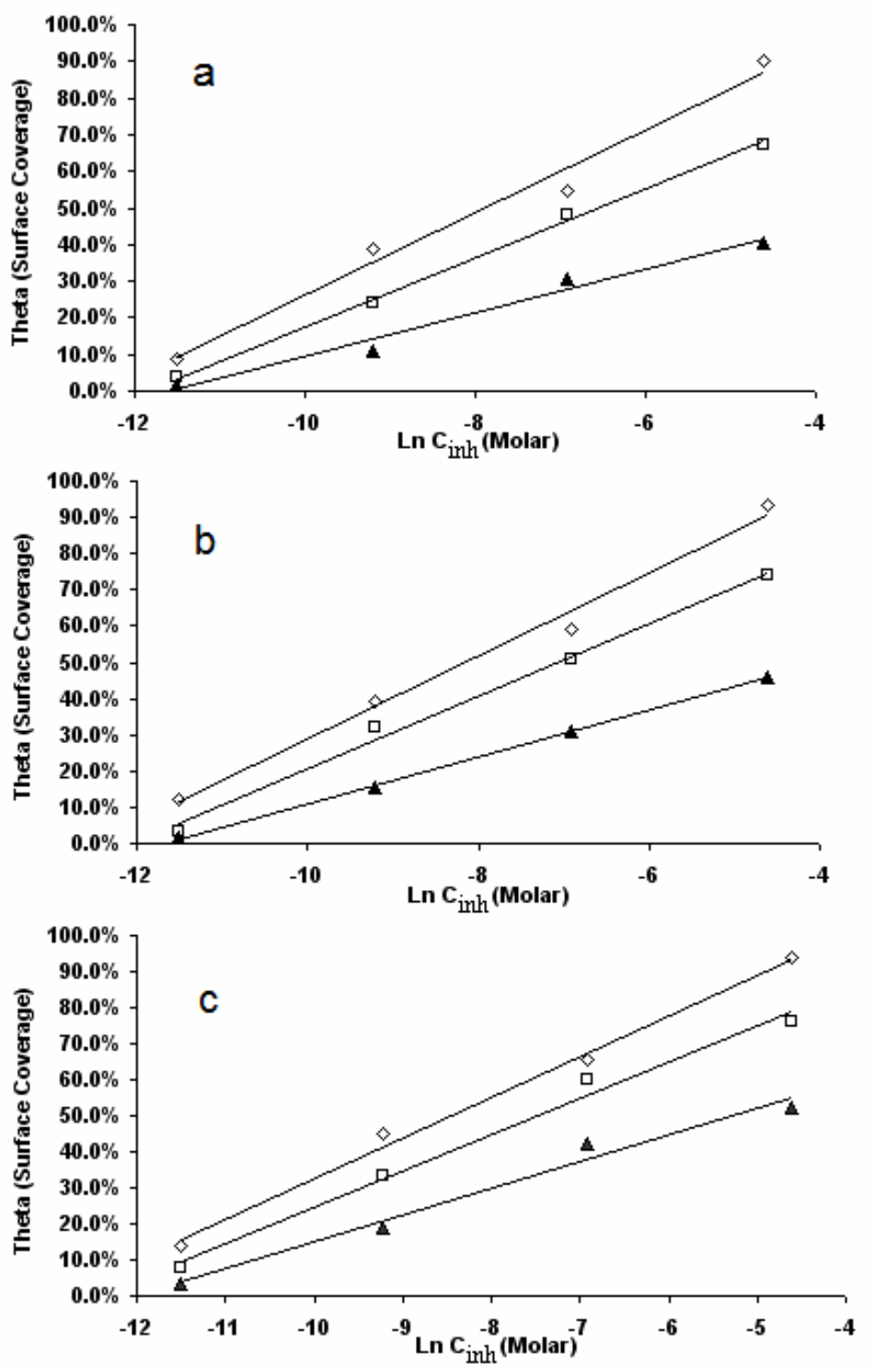

Figure 10: The relationship between surface coverage (θ_C) and Ln (C_{inh}) for 2-MBIM (a), 2-BIM (b) and 2-ABIM (c) at different temperatures; 30 (◊), 40 (□) 50ºC (▲).

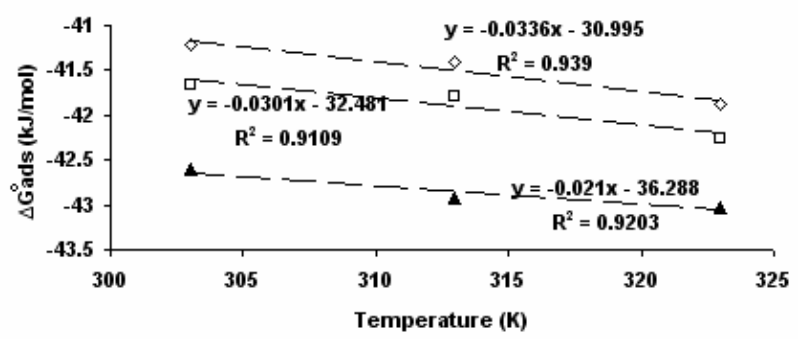

Figure 11: The relationship between ΔG^0_{ads} and temperature for BIM (◊), 2-MBIM (□) and 2-ABIM (▲) based on θ_C calculations.

3.3.3. Comparison between θ_C and θ_R based calculations

The most important thing to know is the mechanism of adsorption. Physisorption and chemisorption or their hybrid can take place during adsorption of the organic molecules to the surface. Many different ways are suggested to evaluate mechanism of adsorption and some of them are as follow:

a. Temperature dependency of inhibition efficiency

Decrease of inhibition efficiency at higher temperatures is related to physisorption [39, 40]. However, inhibition efficiency increase at higher temperatures is linked to chemisorption of adsorbed species after initial physisorption [41]. When physical interactions are involved, decrease of inhibition efficiency is reasonable. Higher kinetic energy of inhibitor molecules can overcome weak interaction of inhibitor with metal surface, thus desorption can take place at higher temperature.

b. Free energy of adsorption

Some investigators [42-45] used free energy of adsorption as a criterion for physisorption and chemisorption. Some authors [42, 43] claimed that when the dominant mechanism is physisorption, the adsorption free energy is less than -20 $kJmol^{-1}$, while free energy of adsorption more negative than -40 $kJmol^{-1}$ indicates chemisorption mechanism.

c. Adsorption enthalpy

Others [45-48] take the adsorption enthalpy as a criterion for adsorption mechanism. They provide a range of adsorption enthalpies as free energy of adsorption to indicate the adsorption mechanism; however, authors are not unanimous in defined ranges.

As can be seen in Table 1, surface coverage declines as temperature increases. This trend is true for both θ_C and θ_R based calculations for physisorption. Free energies of adsorption are all in the range of -41 to -47 $kJmol^{-1}$ whilst adsorption enthalpies (Table 3) are all more positive than -40 $kJmol^{-1}$ in the range of -25.7 to -36.3$kJmol^{-1}$. Adsorption free energy and enthalpy reveals the intermolecular interactions between adsorbate and adsorbent resulting in energy release by reaction. Nevertheless, it should be mentioned that released energy does not always indicate chemical and physical adsorption. Physical adsorption of multifunctional molecules may have more negative enthalpy and free energy than chemisorption of monofunctional molecules [49]. Also, the chemical reaction can take place on a physically attached layer of corrosion products on the surface which does not equal to chemisorption on the electrode surface. It seems that for this case study temperature dependency of inhibition efficiency is the best criterion to identify between physisorption and chemisorption. Considering all above, dominant mechanism of adsorption is physisorption; however, chemical reactions may take place due to ligand substitution reaction of imidazole derivatives with OH^- or H_2O of Fe aqua-hydroxy complexes which can be exist on the surface of corroding mild steel. Calculations resulted in positive ΔS^0_{ads} while for adsorption it is more reasonable to have negative entropy because of decreasing disordering and loss of freedom due to adsorption. It seems that a kind of disordering is taking place, which might be related to decrease of n value of CPE element (Table 1). The parameter "n" of CPE is an indication of electrode surface heterogeneity [31]. The lower the value of “n”, the more heterogeneous is the surface.

Increase of surface heterogeneity may be related to increase of disordering. Positive adsorption entropies have been reported in some literatures [50, 51], however no evidence of disordering have been introduced. Surface heterogeneity parameter extracted by θ_R calculations was around 20 (section 3.3.1) while in the case of θ_C, "f" takes value around 9 (section 3.3.2).

Adsorption energies calculated by θ_R and θ_C generally follow the same trend. However, energies calculated based on θ_C were higher compared to those calculated by θ_R. Regarding to Table 1, in the most cases $\theta_C > \theta_R$. Surface coverage based on resistance represents ability of the adsorbed inhibitors to increase charge transfer resistance and reduce corrosion through surface blocking while surface coverage based on capacitance represents the ability of adsorbed inhibitors to reduce double layer capacity through accumulation on the surface and replacement with water molecules. The plot of θ_C vs θ_R for studied inhibitors are displayed in Figure 12 revealing slope equal to 1.708 which means their ability to accumulate at the electrode-electrolyte interface is more than their ability to block the surface. Many authors [52-54] claimed that inhibition efficiencies calculated by weight loss, polarization or EIS (θ_R) are equal to surface coverage. It seems that at least for mild steel immersed in 3.5% NaCl and inhibited by imidazoles this is not true and more than expected imidazoles are adsorbed on the surface. In other words, for this case study imidazoles are poor blocking agents, despite their adsorption on the surface.

Some reasons could be provided for the big difference between θ_R and θ_C. Orientation of inhibitor molecules at the interface is influential on the surface blocking. They may adsorb on the surface but without parallel orientation on the surface they could not be effective blocking agent. However, according to the Pourbaix diagram of Fe, at neutral condition corrosion products as ferric and ferrous oxides and hydroxides could be formed. Adsorption of the inhibitors on the porous structure of corrosion products may not lead to an efficient surface blocking. Adsorption of inhibitors on the surface rust is studied in section 3.5.

Taking inhibition efficiency equal to surface coverage may result in erroneous results in adsorption isotherm studies. The difference between θ_R and θ_C can be seen in some literatures [55-57]. It can be understood from Table 1 that inhibition efficiency of imidazoles follows the order: 2-ABIM>2-MBIM>BIM. Introduction of an electron donating group in the 2nd position of imidazole ring (Figure 1) can change electron donating power, dipole moment and electronic energy levels. The quantum chemical study can reveal the impact of each factor.

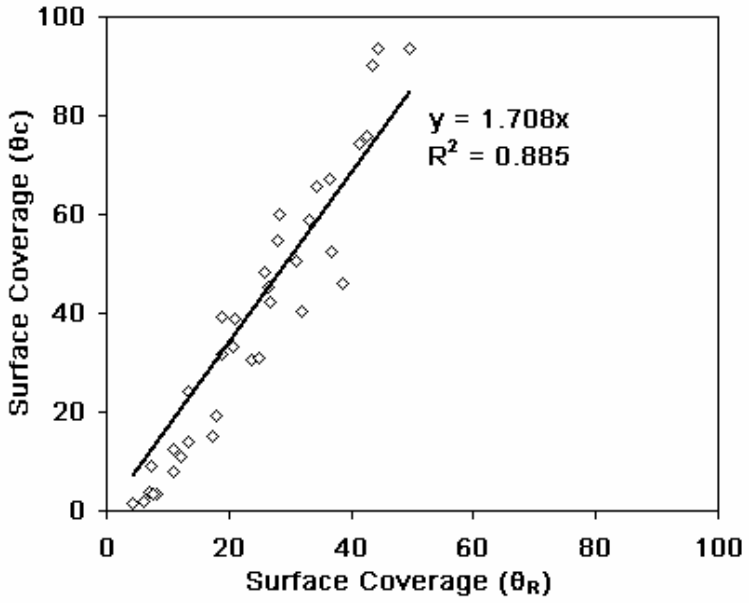

Figure 12: θ_C vs θ_R diagram for the studied imidazole derivatives in 3.5% NaCl solution.

Table 4: The pH of test solutions.

Imidazole Derivatives	pH
BIM	7.5
2-MBIM	8.8
2-ABIM	9.1
Blank	6.0

3.4. pH measurement

The pH-metry results are listed in Table 4 for the test solutions. Introduction of imidazole derivatives resulted in an increase of pH from 6.01 for the Blank solution. Such a behavior could be attributed to the ability of imidazole derivatives to be partially protonated. Table 4 reveals that the ability of imidazole derivatives to adsorb proton follows the sequence: 2-ABIM>2-MBIM>BIM.

As the amino and methyl groups are electron-donating, the basicity of the benzimidazole molecule increases with introduction of these groups in the molecular structure. As the basicity of a molecule increases, the proton affinity and charge on the nitrogen atoms will increase at the same time. The correlations between the calculated proton affinities with the charges on active adsorption sites and inhibition efficiencies are discussed by some authors [58]. The partially protonated species could readily be neutralized by produced OH^- ions in order to form free base with active adsorption sites at cathodic areas. Protonation of imidazole derivatives in solution and deprotonation at cathodic areas maybe the reason of cathodic inhibition of imidazole derivatives as discussed in section 3.2.

The more basic the inhibitor, the higher is the activity and inhibition efficiency. The protonation order is in complete agreement with the inhibition order obtained after 24-hr immersion (section 3.1). However, the inhibition order obtained after 1-hr immersion (section 3.2) could be related to kinetic of deprotonation at cathodic area. Amino group on 2-ABIM could be easily protonated, although deprotonation may take some time to occur.

4. Conclusions

From the results, it could be concluded that:

1. BIM, 2-MBIM, 2-ABIM physically adsorb on the mild steel surface.
2. The inhibition efficiency of imidazoles follows the order: 2-ABIM>2-MBIM> BIM.
3. These compounds act as poor corrosion inhibitors even at high concentrations.
4. The adsorption of used compounds on the steel surface obeys Temkin isotherm.
5. Inhibition efficiencies calculated by change transfer resistance were generally lower than those calculated by double layer capacitance. This means imidazoles adsorbed on the surface more than what charge transfer resistance values estimate. It may be true for the case in which surface coverage (inhibition efficiency) is evaluated by weight loss and DC polarization techniques.
6. Increase of surface heterogeneity may be related to disordering increment which can be identified by the increase of entropy.
7. The pH decline of the solutions containing imidazole derivatives after contact with mild steel sample is related to diminished inhibitor concentration due to adsorption on the surface.
8. The ability of imidazole derivatives to adsorb proton follows the sequence: 2-ABIM>2-MBIM>BIM which has good correlation with the order of their inhibition efficiencies. It seems that the more basic the inhibitor the higher is its activity.

5. References

1. E. Stupnisek-Lisac, A. Gazivoda, M. Madzarac, Evaluation of non-toxic corrosion inhibitors for copper in sulphuric acid, *Electrochim. Acta,* 47 (2002) 4189-4194.
2. A. Khavasfar, M. H. Moayed and M. M. Attar, An Investigation on the performance of an imidazoline based commercial Corrosion inhibitor on CO2 corrosion of gas-well tubing steel by EIS technique, *Iranian J. Mater. Sci. Eng*., 4 (2007), 1-8.
3. O. Benali, L. Larabi, B. Tabti, Y. Harek, Influence of 1-methyl 2-mercapto imidazole on corrosion inhibition of carbon steel in 0.5 M H_2SO_4, *Anti-Corros. Meth. Mater*.,52 (2005) 280-285.
4. J. Morales Roque, T. Pandiyan, J. Cruz, E. Garcia-Ochoa, DFT and electrochemical studies of tris(benzimidazole-2-ylmethyl)amine as an efficient corrosion inhibitor for carbon steel surface, *Corros. Sci.*, 50 (2008), 614-624.
5. G. Bereket, E. Hur, C. Ogretir, Quantum chemical studies on some imidazole derivatives as corrosion inhibitors for iron in acidic medium, *J. Mol. Struct.* 578 (2002), 79-88.
6. J. Shukla, K.S. Pitre, Electrochemical Behavior of Brass in Acid Solutions and the Inhibitive Effect of Imidazole, Corros. Rev., 20, 3 (2002), 217-230.
7. El Sayed H. El Ashry, A. El Nemr, S. A. Essawy, S. Ragab, Corrosion inhibitors part V: QSAR of benzimidazole and 2-substituted derivatives as corrosion inhibitors by using the quantum chemical parameters, *Prog. Org. Coat,*. 61 (2008), 11-20.
8. M. H. Wahdan, G. K. Gomma, Effect of copper cation on electrochemical behaviour of steel in presence of imidazole in acid medium, *Mater. Chem. Phys.,* 47 (1997), 176-183.
9. S. Muralidharan, S. Venkatakrishna Iyer, The influence of N-heterocyclics on corrosion inhibition and hydrogen permeation through mild steel in acidic solutions, *Anti-Corros. Meth. Mater,*. 44 (1997), 100-106.
10. A. Popova, M. Christov, A. Zwetanova, Effect of the molecular structure on the inhibitor properties of azoles on mild steel corrosion in 1 M hydrochloric acid, *Corros. Sci.,* 49 (2007), 2131-2143.
11. A. Popova, Temperature effect on mild steel corrosion in acid media in presence of azoles, Corro*s. Sci.,* 49 (2007) 2144-2158
12. D. Wahyuningrum, S. Achmad, Y. Maolana Syah, Buchari, Bunbun Bundjali, B. Ariwahjoedi, The correlation between structure and corrosion inhibition activity of 4, 5-diphenyl-1-vinylimidazole derivative compounds towards mild steel in 1% NaCl solution, *Int. J. Electrochem. Sci.,* 3 (2008), 154-166.
13. H. Amar, A. Tounsi, A. Makayssi, A. Derja, J. Benzakour, A. Outzourhit, Corrosion inhibition of Armco iron by 2-mercaptobenzimidazole in sodium chloride 3% media, *Corros. Sci.*, 49 (2007), 2936-2945.
14. A. Y. El-Etre, Inhibition of C-steel corrosion in acidic solution using the aqueous extract of zallouh root, *Mater. Chem. Phys.,* 108 (2008), 278-282.
15. O. K. Abiola, Adsorption of 3-(4-amino-2-methyl-5-pyrimidyl-methyl)-4-methyl-thia-zolium chloride on mild steel, *Corros. Sci.,* 48, 10 (2006), 3078-3090.
16. M. A. Deyab, H. A. Abo Dief, E. A. Eissa and A. R. Taman, Electrochemical investigations of naphthenic acid corrosion for carbon steel and the inhibitive effect by some ethoxylated fatty acids, *Electrochim. Acta*, 52 (2007), 8105-8110.
17. M. N. H. Moussa, A. A. El-Far and A. A. El-Shafei, The use of water-soluble hydrazones as inhibitors for the corrosion of C-steel in acidic medium, *Mater. Chem. Phys.*, 105 (2007), 105-113.
18. E. E. Oguzie, Corrosion inhibition of aluminium in acidic and alkaline media by Sansevieria trifasciata extract, *Corros. Sci.,* 49 (2007), 1527-1539.
19. J. O. M. Bockris, Sh. U. M. Khan, Surface Electrochemistry, Springer, 1993, p. 199.
20. W. J. Thomas, B. D. Crittenden, Adsorption Technology and Design, Butterworth-Heinemann, 1998, p. 42.
21. K. F. Khaled, Molecular simulation, quantum chemical calculations and electrochemical studies for inhibition of mild steel by triazoles, *Electrochim. Acta,* 53 (2008), 3484-3492.
22. R. Rosliza, W. B. Wan Nik, H. B. Senin, The

effect of inhibitor on the corrosion of aluminum alloys in acidic solutions, *Mater. Chem. Phys.*,107 (2008), 281-288.

23. X. Li, S. Deng, G. Mu, H. Fu, F. Yang, Inhibition effect of nonionic surfactant on the corrosion of cold rolled steel in hydrochloric acid, *Corros. Sci.,* 50 (2008), 420-430.
24. E. Alibakhshi, E. Ghasemi, M. Mahdavian, A Comparison Study on Corrosion Behavior of Zinc Phosphate and Potassium Zinc Phosphate Anticorrosive Pigments, *Prog. Color Colorants Coat.,* 5 (2012), 91-99.
25. A. Ghanbari, M. M. Attar, M. Mahdavian, Acetylacetonate Complexes as New Corrosion Inhibitors in Phosphoric Acid Media: Inhibition and Synergism Study, *Prog. Color Colorants Coat.,* 2 (2009), 115-122.
26. A. Ghanbari, M. M. Attar , Mild Steel Surface Pretreatment Using Phosphoric acid-Inhibitor Solution, *Prog. Color Colorants Coat.,* 7 (2014), 269-284.
27. S. Lajevardi Esfahani, Z. Ranjbar, S. Rastega, Evaluation of Anticorrosion Behavior of Automotive Electrocoating Primers by the AC-DC-AC Accelerated Test Method, *Prog. Color Colorants Coat.,* 7 (2014), 187-199.
28. B. Ramezanzadeh, M. Mehdipour, S. Y. Arman, Application of Electrochemical Noise to Investigate Corrosion Inhibition Properties of Some Azole Compounds on Aluminum in 0.25 M HCl, *Prog. Color Colorants Coat.*, 8 (2015) 69-86.
29. M. S. Morad, Inhibition of iron corrosion in acid solutions by Cefatrexyl: Behaviour near and at the corrosion potential, *Corros. Sci.,* 50 (2008), 436-448.
30. E. Machnikova, K. H. Whitmire, N. Hackerman, Corrosion inhibition of carbon steel in hydrochloric acid by furan derivatives, *Electrochim. Acta,* 53 (2008), 6024-6032.
31. V. Mei-Wen Huang, V. Vivier, I. Frateur, M. E. Orazem, B. Tribolletb, The Global and Local Impedance Response of a Blocking Disk Electrode with Local Constant-Phase-Element Behavior, *J. Electrochem. Soc.,* 154 (2007), 89-98.
32. M. Schutze, Materials Science and Technology:Vol. I, Wiley-VCH Verlag GmbH, 2000.
33. Y. Feng, S. Chen, H. Zhang, P. Li, L. Wu, W. Guo, Characterization of iron surface modified by 2-mercaptobenzothiazole self-assembled monolayers, *Appl. Surf. Sci.,* 253 (2006), 2812-2819.
34. M. Motamedi, A.R. Tehran-bagha, M. Mahdavian, A comparative study on the electrochemical behavior of mild steel in sulfamic acid solution in the presence of monomeric and gemini surfactants, *Electrochim. Acta*, 58 (2011), 488-496.
35. Y. Abboud, A. Abourriche, T. Saffaj, M. Berrada, M. Charrouf, A. Bennamara, A. Cherqaoui, D. Takky, The inhibition of mild steel corrosion in acidic medium by 2,2′-bis(benzimidazole), *Appl. Surf. Sci.,* 252 (2006), 8178-8184.
36. P. Morales-Gil, G. Negron-Silva, M. Romero-Romo, C. A ngeles-Chavez, M. Palomar-Pardave, Corrosion inhibition of pipeline steel grade API 5L X52 immersed in a 1 M H_2SO_4 aqueous solution using heterocyclic organic molecules, *Electrochimica Acta*, 49 (2004), 4733-4741.
37. A. Popova, M. Christov, A. Zwetanova, Effect of the molecular structure on the inhibitor properties of azoles on mild steel corrosion in 1M hydrochloric acid, *Corros. Sci.,* 49 (2007), 2131-2143.
38. A. Popova, M. Christov, S. Raicheva, E. Sokolova, Adsorption and inhibitive properties of benzimidazole derivatives in acid mild steel corrosion, *Corros. Sci.,* 46 (2004), 1333-1350.
39. A.Y. El-Etre, Inhibition of aluminum corrosion using Opuntia extract, *Corros. Sci.,* 45 (2003), 2485-2495.
40. S. A. Ali, A. M. El-Shareef, R. F. Al-Ghamdi, M. T. Saeed, The isoxazolidines: the effects of steric factor and hydrophobic chain length on the corrosion inhibition of mild steel in acidic medium, *Corros. Sci.,* 47 (2005), 2659-2678.
41. M. Lebrini, M. Lagrenee, H. Vezin, L. Gengembre, F. Bentiss, Electrochemical and quantum chemical studies of new thiadiazole derivatives adsorption on mild steel in normal hydrochloric acid medium, *Corros. Sci.,* 47 (2005), 485-505.
42. F. Kellou-Kerkouche, A. Benchettara, S. Amara, Effect of sodium dodecyl benzene

sulfonate on the corrosion inhibition of Fe-1Ti-20C alloy in 0.5 M H_2SO_4, *Mater. Chem. Phys.,* 110 (2008), 26-33.

43. R. Hasanov, M. Sadıkoglu, S. Bilgic, Electrochemical and quantum chemical studies of some Schiff bases on the corrosion of steel in H2SO4 solution, *Appl. Surf. Sci.,* 253, 8 (2007), 3913-3921.
44. P. Somasundaran, Encyclopedia of Surface and Colloid Science, CRC Press, 2006.
45. L. Tang, X. Li, G. Mu, L. Li, G. Liu, Synergistic effect between 4-(2-pyridylazo) resorcin and chloride ion on the corrosion of cold rolled steel in 0.5 M sulfuric acid, *Appl. Surf. Sci.,* 252 (2006), 6394-6401.
46. B. Bhushan, Principles and applications of tribology, Wiley-IEEE, 1999.
47. L.L. Shreir, G.T. Burstein, R.A. Jarman, Corrosion, Butterworth-Heinemann, 1994.
48. M. E. Davis, R. J. Davis, Fundamentals of Chemical Reaction Engineering, McGraw-Hill Professional, 2002.
49. T. Hubbard, Encyclopedia of Surface and Colloid Science: A-Dif, CRC Press, 2002, p. 608.
50. M. Bouklah, B. Hammouti, M. Lagrenee b, F. Bentiss, Thermodynamic properties of 2,5-bis(4-methoxyphenyl)-1,3,4-oxadiazole as a corrosion inhibitor for mild steel in normal sulfuric acid medium, *Corros. Sci.,* 48 (2006), 2831-2842.
51. F. Bentiss, M. Lebrini, M. Lagrenee, Thermodynamic characterization of metal dissolution and inhibitor adsorption processes in mild steel/2,5-bis(n-thienyl)-1,3,4-thiadiazoles/hydrochloric acid system, *Corros. Sci.,* 47 (2005), 2915-2931.
52. X. Li, L. Tang, G. Mu, L. Li, G. Liu, The synergistic inhibition of the cold rolled steel Corrosion in 0.5 M sulfuric acid by the mixture of OP and bromide ion, Mater. Lett., 61 (2007), 2723-2727.
53. H. Amar, J. Benzakour, A. Derja, D. Villemin, B. Moreau, T. Braisaz, Piperidin-1-yl-phosphonic acid and (4-phosphono-piperazin-1-yl) phosphonic acid: A new class of iron corrosion inhibitors in sodium chloride 3% media, *Appl. Surf. Sci.,* 252 (2006), 6162-6172.
54. G. K. Gomma, Effect of azole compounds on corrosion of copper in acid medium, *Mater. Chem. Phys.,* 56 (1998), 27-34.
55. N. Huynh, S. E. Bottle, T. Notoya, A. Trueman, B. Hinton and D. P. Schweinsberg, Studies on alkyl esters of carboxybenzotriazole as inhibitors for copper corrosion, Corros. Sci. 44, 6 (2002), 1257-1276.
56. S. A. Ali, H. A. Al-Muallem, M. T. Saeed, S. U. Rahman, Hydrophobic-tailed bicycloisoxazolidines: A comparative study of the newly synthesized compounds on the inhibition of mild steel corrosion in hydrochloric and sulfuric acid media, *Corros. Sci.,* 50 (2008), 664-675.
57. R. A. Prabhu, T. V. Venkatesha, A. V. Shanbhag, B. M. Praveen, G. M. Kulkarni, R. G. Kalkhambkar, Quinol-2-thione compounds as corrosion inhibitors for mild steel in acid solution, Mater. Chem. Phys., 108 (2008) 283-289.
58. C. Ogretir, B. Mihci, G. Bereket, Quantum chemical studies of some pyridine derivatives as corrosion inhibitors, *J. Mol. Struct.,* 488 (1999), 223-231.